Networks of Motoneurons with Mixed-Mode Oscillations

Arturo Leos Zamorategui[1]

Centre for Complexity Science, Zeeman Building, University of Warwick, Coventry CV4 7AL, UK

Abstract

In this paper we study the role of Mixed-Mode Oscillations (MMOs), observed experimentally in motoneurons, in the dynamics of different networks. As control parameters we have the applied current (I_{app}) and the coupling strength (G_{gap}) between pairs of neurons. By fixing the value of one of these parameters, we analyze the dynamics in the network with identical neurons via a synchrony measure (χ^2) which gives the average fluctuations in the voltage with respect to the fluctuations in the voltage of single cells. To do so, we first compare the synchrony measure with the number of cells given a global coupling. Secondly, we compare χ^2 with the number of connections among cells by changing the number of kth nearest neighbors. Finally, we look at small-world topologies to observe the dependance of χ^2 on the randomness in the network. We also analyze the dynamics of a network with neurons in different regimes, these examples show the importance of mixed-mode oscillations in the overall behavior.

Key words: Networks, motoneurons, mixed-mode oscillations, synchronization

1. Introduction

The stimuli we receive from the external world are processed by our sensory systems creating our own representation of this world. This information guides the motor systems to interact with our environment: from somatic reflexes such as the withdrawal of a finger from the stove, the posture, rythmic patterned motor movements such as walking, to voluntary and complex movements as catching a ball, or even speech. The motor systems within the central nervous system (CNS) are hierarchically organized into (1) the spinal cord, (2) brainstem, and (3) cerebral cortical levels [1]. The *spinal cord level* is mainly involved in reflex responses. The *brainstem level* involves the descending motor pathways from the cerebral cortex that regulate the motor activity of the reflex circuits. At the highest level is the *cerebral cortex* which stimulates both the brainstem and the spinal cord that activate skilled movements such as writting.

The somatic reflexes are the automatic stereotypic motor responses by voluntary muscles to sensory stimuli. Since the body is continuously bombarded by internal and external stimuli, a selection must be made by sensory receptors within the skin, voluntary muscles, tendons, and joints. From them a signal is transmitted via spinal and cranial sensory nerves to the spinal cord and brainstem for processing in order to respond. This information is conveyed by *alpha motoneurons* to the extrafusal muscle fibers and via *gamma motoneurons* to the intrafusal muscle fibers. The alpha and gamma motoneurons, called lower motoneurons, are the final common pathway to control reflex, postural, rythmic and voluntary movements. The activities of such alpha and gamma motoneurons are affected by multiple receptors from the spinal and cranial nerves and from upper motoneurons which can convey either excitatory or inhibitory signals. These descending pathways are regulated directly or indirectly by the cerebral cortex and the cerebellum [1].

Email address: A.Leos-Zamorategui@warwick.ac.uk (Arturo Leos Zamorategui)

A lesion in the nervous system or a neurologic disease can be manifested by *negative signs* where a loss of a function or capacity is expressed or by *positive signs* which are abnormal motor responses such as Parkinson's disease. These last symptoms appear generally due to the withdrawal of inhibitory influences. Depending on the region affected, we can refer to lesions in the lower motoneurons or upper motoneurons since the symptoms can be easily identified. When lower motoneurons innervating a muscle or a group of muscles results in a paralysis or paresis (partial paralysis, weakness) of those muscles. This occurs in poliomyelitis where the polio virus can selectively affect motoneurons of the spinal cord and of the brainstem. On the contrary, lesions in upper motoneurons can generate multiple symptoms affecting limbs and tendon reflexes as in the paraplegia where a trauma causes a loss in neural activity and paralysis of both lower limbs. Sensations from the body below the affected limbs are absent. In Quadriplegia all of the four limbs are paralysed and it can even affect the control of the diafragm [2].

A little is known about the cause of the Amyotrophic lateral sclerosis also known as motor neuron disease since it is the most common degenerative motor disease. Because there is degeneration of both the upper and lower motoneurons, signs of both types of motoneurons are expressed. Most of the affected muscles show signs of degeneration of lower motoneurons such as paralysis, atrophy, fasciculations, and weakness. Some muscles exhibit signs of upper motoneurons paralysis although these signs are source of controversy [2, 3] and references therein. The degenerative processes include changes in the cell body and in the nerve fibers including breakdown of the myelin sheath and axon in the vicinity of the injury [1].

Loss of neurons occurs normally throughout life. This neuronal loss is generally accompanied by a compensatory sprouting of axonal branches by other CNS neurons in the vicinity, however this is not enough to stop a degenerative process in the CNS. Neurons of fetal and neonatal mammals have a great capacity of regeneration, in consequence transplanting young neurons seems to attain some functional recovery. These techniques, together with new bioengineering techniques that include microsurgical reattachment can be part of the treatment of some degenerative motoneuron disorders [4].

A peculiar characteristic of motoneurons is that they present mixed mode oscillations (MMOs), where low-amplitude high-frequency oscillations alternate with high-amplitude low-frequency spikes. Experimentally it is difficult to observe MMOs since low-amplitude oscillations disappear for motoneurons with high excitability. It is still unknown which ionic currents are responsible for the oscillations and shape the discharge in the subprimary range [5]. MMOs have also been reported in interneurons [6] and pyramidal cells of the frontal cortex [7] and in some cases they were associated with a subthreshold resonance due to a slowly activated potassium current and enhanced by the persistent sodium current [7]. The model we use in this project was first introduced to describe mouse motoneurons [8] where it is argued that the frequency resonance is too low in this kind of motoneurons to explain the high frequency of oscillations. Thus, MMOs in mouse motoneurons are not related to the subthreshold resonance but to the spiking mechanism and arise from the balance between the delayed rectifier current and the sodium current.

To elucidate the role of MMOs in the nervous system we study networks of motoneurons with MMOs coupled via gap junctions in different topologies. A similar work has studied networks of globally coupled inhibitory interneurons that show MMOs, however as we explained above, these oscillations are produced by different mechanisms such as the slow potassium current. It is interesting to mention that in this work, neurons present both clustering and synchronization due to the gap junctions and to the intrinsic dynamics of the neurons [9]. Other studies have considered chemical coupling finding clustering with strong coupling [10].

We focus our attention on electrical coupling via gap junctions, since it is the simplest form of coupling. This coupling plays an important role in coordination and generation of motor outputs [11]. In general, gap junctions among motoneurons will tend to synchronyze their firing which in many cases is a desirable output as in the cardiac muscle or in the respiratory system. In reflex and voluntary movements, it is expected that motoneurons fire simultaneously so that the muscle or groups of muscles contract (or stretch) strongly enough, i.e. when motoneurons fire simultaneously, that increase the amplitude of the

motor output.

In this project we study the dynamics of motoneurons coupled via gap junctions with different topologies. This allows us to understand the role of MMOs in the overall dynamics on the network. To start with, in Section 2 we present the model of a single neuron with three voltage-gated variables and the reduced model which lumps together the sodium conductance inactivation h and the delayed rectifier activation variable n in a single recovery variable W [5]. We also include the bifurcation diagram that shows the voltage of the stationary solution, both the stable and unstable, as a function of the parameter I_{app}. Three region are identified: a quiescent region, a subprimary regime and a primary regime. At the end of this section we introduce the coupling term among neurons in the networks studied and a synchrony measure χ^2 that allows us to describe the dynamics of the network in terms of the fluctuations in the voltage of the neurons. Section 3 shows the numerical results. We analyze first globally coupled networks to understand the influence of the coupling strength G_{gap} and the applied current I_{app} on the overall dynamics. Aditionally, we look at networks in which neurons are linked to their kth nearest neighbors and networks with small-world topologies. We conclude this section by showing some examples in which neurons within the network are in different regimes. Section 4 is concerned with the discussion of the results.

2. Model

The initial model for one uncoupled neuron is given by a set of four differential equations with two fast currents that generate spikes given by the inactivation function of sodium current h and the delayed rectifier potassium conductance n and the slower afterhyperpolarization (AHP) conductance [5]. The sodium conductance is assumed to activate instantaneously and to inactivate fast. This equations read as follows:

$$C_m\frac{dV}{dt} = I_L(V) + I_{Na}(V,h) - I_K(V,n) + I_{AHP}(V,z) + I_{app}(t), \tag{1}$$

$$\tau_h\frac{dh}{dt} = h_\infty(V) - h, \tag{2}$$

$$\tau_n\frac{dn}{dt} = n_\infty(V) - n, \tag{3}$$

$$\tau_z(V)\frac{dz}{dt} = z_\infty(V) - z. \tag{4}$$

2.1. *Reduced model*

In order to analyze these equations mathematically it is convenient to reduce this model to a system of three variables. To do so, both the sodium conductance inactivation h and the delayed rectifier activation variable n, Eqs. (2) and (3) respectively, are replaced by the potentials W_h and W_n via the change of variable $h = h_\infty(W_h)$ and $n = n_\infty(W_n)$ and then W_h and W_n are replaced by W as explained in [5]. The reduced model is then given by

$$C_m\frac{dV}{dt} = G_L(V_L - V) + G_{Na}m_\infty(V)^3h_\infty(W)(V_{Na} - V) - G_Kn_\infty(W)(V_K - V) + G_{AHP}z(V_{AHP} - V) + I_{app}, \tag{5}$$

$$\frac{dW}{dt} = \frac{\gamma_h(V,W)}{\gamma_h(V,W)+\gamma_n(V,W)}\frac{h_\infty(V) - h_\infty(W)}{\tau_h dh_\infty(W)/dW} + \frac{\gamma_n(V,W)}{\gamma_h(V,W)+\gamma_n(V,W)}\frac{n_\infty(V) - n_\infty(W)}{\tau_n dn_\infty(W)/dW}, \tag{6}$$

$$\tau_z(V)\frac{dz}{dt} = z_\infty(V) - z. \tag{7}$$

In Eqs. (5) and (6) the voltage-gated variables are

$$m_\infty(V) = \frac{1}{1+e^{-(V+46)/10}},$$
$$h_\infty(V) = \frac{1}{1+e^{(V+70)/10}},$$
$$n_\infty(V) = \frac{1}{1+e^{-(V+40)/10}}.$$

In Eq. (6), the functions $\gamma_h(V,W)$ and $\gamma_n(V,W)$ are defined as follows

$$\gamma_h(V,W) = \frac{\partial I_{Na}}{\partial h_\infty}\frac{dh_\infty}{dW}$$

and

$$\gamma_n(V,W) = \frac{\partial I_K}{\partial n_\infty}\frac{dn_\infty}{dW}.$$

In Eq. (7), the activation variable of the AHP conductance z is such that when a spike takes place, its value varies as $z_{after} = \alpha \cdot z_{before} + (1-\alpha)$, where $0 \leq \alpha \leq 1$ and then it decays exponentially according to $z(t) = z_{after}\, e^{-t/\tau_z}$. The values of the parameters are summarized in the table below.

Na current	**K current**	**AHP current**	**Others**
$V_{Na} = 50$ mV	$V_K = -80$ mV	$V_{AHP} = V_K$mV	$V_L = -80$ mV
$G_{Na} = 50\,\mu$S	$G_K = 7\,\mu$S	$G_{AHP} = 0.7\,\mu$S	$G_L = 0.3\,\mu$S
$\tau_h = 1.0$ ms	$\tau_n = 1.0$ ms	$\tau_{zmax} = 10$ ms	$C_m = 0.8$ nF

This model produces MMOs which are due to the balance between the spike-generating currents [5]. For example, it is observed that either adding a persistent component to the sodium current or a decrease of the delayed rectifier current reduces MMOs. Subthreshold oscillations (STOs) can even disappear when the transient sodium conductance is increased beyond $60\,\mu$S. The greater the membrane excitability, the fewer STOs are observed, i.e. MMOs require low membrane excitability.

The AHP current interacts with the slow inactivation of the sodium current to control the excitability and consequently, the firing pattern. The AHP reduces the firing frequency yet it favors primary range firing because it increases the motoneuron excitability by de-inactivating the sodium current.

In order to identify the neurons within the network we label the state variables V_i, W_i and z_i. Additionally, we add a *coupling term* I_{gap} to Eq. (5) corresponding to the gap junctions among neurons in the network

$$I_{gap,i} = \frac{G_{gap}}{N}\sum_{i=1}^{N} A_{ij}(V_j - V_i),$$

where A_{ij} is the adjacency matrix whose entries are $a_{ij} = 1$ if neuron i is coupled to neuron j and it is zero otherwise.

*2.2. **Mathematical analysis of the reduced single-cell model***

The fixed points of this model are located in the $z = 0$ plane and the intersections of the nullclines $dV/dt = 0$ and $dW/dt = 0$. The second nullcline is the straigh line $V = W$. Therefore, the fixed points are given by the steady-state current voltage equation (5), as follows

$$G_L(V_L - V) + G_{Na}m_\infty(V)^3 h_\infty(V)(V_{Na} - V) - G_K n_\infty(V)(V_K - V) + G_{AHP}z(V_{AHP} - V) + I_{app} = 0.$$

The bifurcation diagram of the model in Fig. 1 shows the voltage of the stationary solution, both the stable and unstable, as a function of the parameter I_{app}. Three regions are identified: (a) in the quiescent regime,

the model shows a stable fixed point and oscillations die out. (b) This fixed point becomes unstable when it merges with an unstable limit cycle at $I_{app} \approx 4.1$ nA through a subcritical Hopf bifurcation. Small amplitude oscillations (STOs) around the unstable fixed point alternate with large amplitude spikes. As the applied current increases, the inter-spike period decreases. Figure 2 show the voltage traces and the trajectory in the phase space for different values of the current in this regime. (iii) At $I_{app} \approx 7.3$ nA, the subthreshold oscillations and the unstable periodic solution disappear and the neuron fires with a fixed frequency.

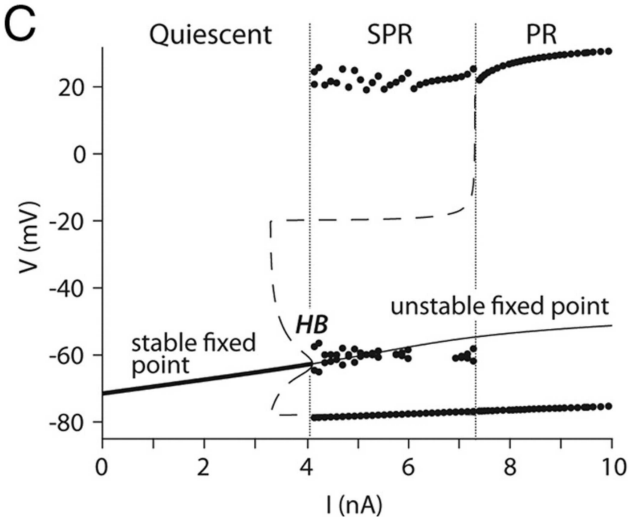

Figure 1: Bifurcation diagram of the reduced model (Eqs. (5)-(7)) shows the voltage of the stationary solution, both the stable and unstable, as a function of the parameter I_{app}. Three regions are identified: (a) in the quiescent regime, the model shows a stable fixed point and oscillations die out. (b) This fixed point becomes unstable when it merges with an unstable limit cycle at $I_{app} \approx 4.1$ nA through a subcritical Hopf bifurcation. (iii) At $I_{app} \approx 7.3$ nA, the subthreshold oscillations and the unstable periodic solution disappear and the neuron fires with a fixed frequency. [5]

2.3. ***Synchrony measure in a network***

In order to measure the fluctuations in the voltage of the neurons within a network it is necessary to compute the variance of their values for many iterations so that we are able to recognize a network that completely synchronizes from a network that either form clusters or does not synchronize at all. The synchrony measure used to analyze the dynamics in the networks we look at was introduced first in an attempt to measure the correlations in neural networks [12, 13, 14, 15]. Given the average voltage

$$V(t) = \frac{1}{N}\sum_{i=1}^{N} V_i(t),$$

the variance of the time fluctuations is given by [15]

$$\sigma_V^2 = \langle [V(t)]^2 \rangle_t - [\langle V(t) \rangle_t]^2 \,,$$

where $\langle \cdot \rangle = (1/T)\int_0^T \cdot \, dt$ denotes the time-averaging over a time T. To normalize σ_V^2 we calculate fluctuations over single cell potentials

$$\sigma_{V_i}^2 = \langle [V_i(t)]^2 \rangle_t - [\langle V_i(t) \rangle_t]^2 \,.$$

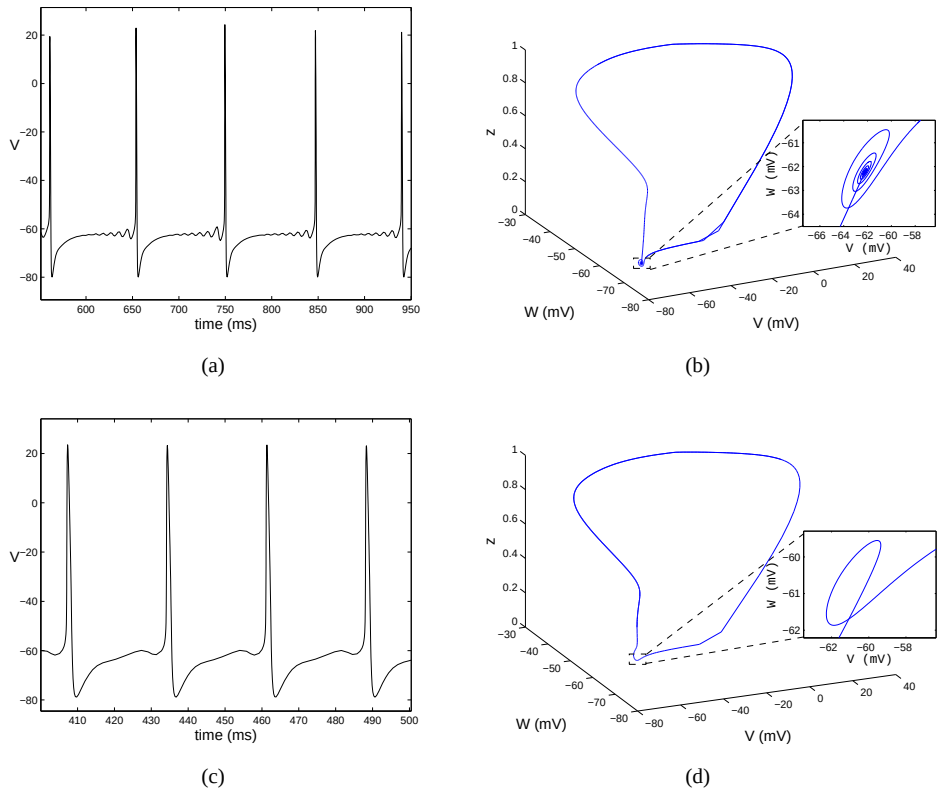

Figure 2: Voltage traces and trajectories in the phase space for two neurons (a), (b) $I_{app} = 4.3$ nA and (c), (d) $I_{app} = 6.0$ nA. The phase space in (b) shows oscillations (STOs) around the unstable fixed point before the spike takes place. Inset: Projection on the plane $z = 0$ of the STOs around the unstable fixed point. In (d) one oscillation around the unstable fixed point is observed. Inset: Projection on the plane $z = 0$ of the STO around the unstable fixed point.

The synchrony measure is then given by the expression

$$\chi^2(N) = \frac{\sigma_V^2}{\frac{1}{N}\sum_{i=1}^{N}\sigma_{V_i}^2}, \tag{8}$$

which takes values between 1 and 0 with 1 when the network is completely synchronyzed in the sense that all states variables are equal for all neurons or 0 if the cells are spiking randomly which does not happen since we are not adding noise.

3. Results

3.1. ***Globally coupled networks***

Our first example consists of globally coupled neurons. The regularity of such networks allows us to focus our attention on the control parameters G_{gap} and I_{app}. Since all the neurons in the network are coupled all-to-all, the topology in this case does not take a main role in the dynamics of the network.

3.1.1. χ^2 ***vs*** G_{gap}

We first analyze the relationship between the synchrony measure χ^2 as expressed in Eq. (8) as a function of the coupling strength G_{gap} for networks with 2, 6 and 10 identical neurons keeping the applied current I_{app} constant as shown in Fig. 3. Two cases are studied: (a) $I_{app} = 4.5$ nA (Fig. 3(a)) and (b) $I_{app} = 6.0$ nA (Fig. 3(b)). For each point, we average 20 realizations with random initial conditions where each realization runs for 30000 iterations with a time step of $dt = 0.05$ ms. Fig. 2(a) shows the voltage trace for a neuron in the regime treated in case (a), a cell in this regime presents many STOs before a spike is produced. Similarly, Fig. 2(c) shows the voltage trace of a cell in the regime studied in case (b), one single STO is observed before the neuron fires.

Let us first look at the case (a). We can see that the slope changes with the coupling strength, above $G_{gap} = 0.002$ μS becomes more likely that two neurons synchronize. Equivalently to this interpretation, we can also say that the speed at which two neurons synchronize is faster as we increase G_{gap} beyond 0.002 μ and until around 0.008 μS. For a value to reach $\chi^2 = 1$ in a transient time less or equal to 10000 iterations, the coupling strength has to be extremely high for the system to approach assymptotically to the value $\chi^2 = 1$. For 6 neurons we observe a similar behaviour until $G_{gap} = 0.0065$ μS. However, increasing the coupling strength beyond this value produces more fluctuations and therefore a smaller value of the synchrony measure. The same occurs to a network with 10 neurons but for higher coupling strength.

For a current $I_{app} = 6.0$ nA in the case (b), a slight increase in the coupling strength from $G_{gap} = 0.001$ μS demonstrates that neurons reach the stable state (clustering or complete synchronization) considerably faster. The same asymptotic behaviour is observed, nevertheless.

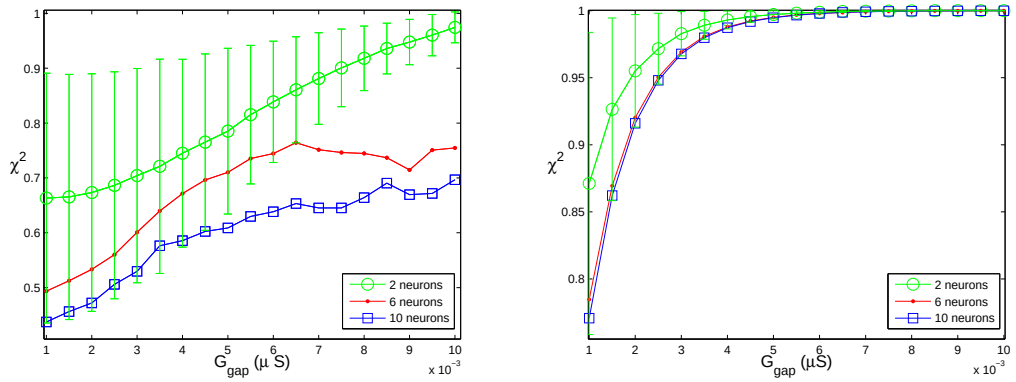

Figure 3: χ^2 vs G_{gap} for globally coupled networks with different number of neurons (line is used for reference only). (a) For $I_{app} = 4.5$ nA the fluctuations are higher and consequently the network reaches the state χ^2 more slowly. For 6 and 10 neurons is not even clear if such a state is reached for strong enough coupling. (b) For $I_{app} = 6.0$ nA the functional dependence of χ^2 on the coupling strength G_{gap} is evident, and the behaviour is the same for networks with different number of neurons yet the more neurons are, the faster the convergence is. Each value has been averaged over 15 realizations where each of them runs 30000 iterations with a transient time of 10000. In order to show the data more clearly we just include error bars for two neuron networks.

The difference in subprimary oscillations in these two regimes considered above completely changes the dynamics in the network. The presence of MMOs, as we discuss later, generates a richer dynamics for which we cannot just find a synchronized state where all neurons fire together but also clusters of neurons where cells within a cluster fire simulatenously. When these clusters are observed (figure not included), MMOs determine the difference in phase between clusters.

3.1.2. χ^2 *vs* I_{app}

Fig. 4 shows the relationship between the synchrony measure χ^2 and the applied current I_{app} by fixing the coupling strength to $G_{gap} = 0.006$ μS. Interestingly, for some values of the applied current the network synchronizes more slowly independently of the number of neurons in the network. For example, at $I_{app} = 5.0$ nA the network does not reach the synchronized state (for which $\chi^2 = 1$) within the 30000 iterations that the simulations last even though for the previous value $I_{app} = 4.9$ nA and the next value $I_{app} = 5.1$ nA such synchronized state is reached. We might explain this due to the difference in the number of MMOs, however this is not the case here since those three cases present one subprimary oscillation. Therefore, it is not clear what determines such a slow behaviour for some currents.

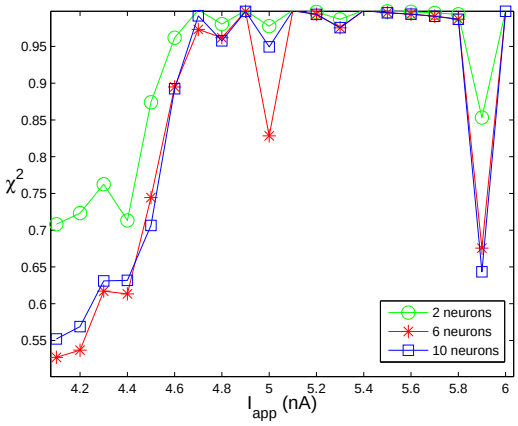

Figure 4: χ^2 vs I_{app} for globally coupled networks with different number of neurons and $G_{gap} = 0.006$ μS (line is used for reference only). For some values of the current the networks apparently do not synchronize, however single realizations show the opposite. This is due to the speed at which the network reaches the state $\chi^2 = 1$; interestingly for some values of the current it takes longer. Each value has been averaged over 15 realizations where each of them runs 30000 iterations with a transient time of 10000.

3.2. *k**th nearest neighbors networks***

In this example we analyze the influence of regular topologies in the dynamics of the networks by looking at the relationship between the synchrony measure χ^2 and the parameter G_{gap} by fixing the number of neurons in the networks and varying the number of neighbors to which a neuron is linked. We focus on networks with 10 neurons connected to their 1st, 2nd and 3rd nearest neighbors.

We consider two cases: (a) $I_{app} = 4.5$ nA (Fig. 5(a)) and (b) $I_{app} = 6.0$ nA (Fig. 5(b)). In the first case, the fluctuations are higher due to the MMOs. For 2nd nearest neighbors it is expected that the network will synchronize for strong enough coupling however, it is not easy to claim the same for 3rd nearest neighbors since beyond $G_{gap} = 0.0075$ μS the fluctuations in χ^2 are higher and its convergence to 1 is not evident. For the second case, there is a clear relationship between χ^2 and G_{gap}. As the coupling strength increases, χ^2 tends asymptotically to 1 which is the completely synchronized state. The speed at which such a state is reached is directly related to the number of neighbors.

3.3. ***Small-world networks***

The last example with identical neurons, i.e. with all the neurons in the same regime, studies the relationship between the synchrony measure χ^2 with the coupling strength G_{gap} and the applied current I_{app}

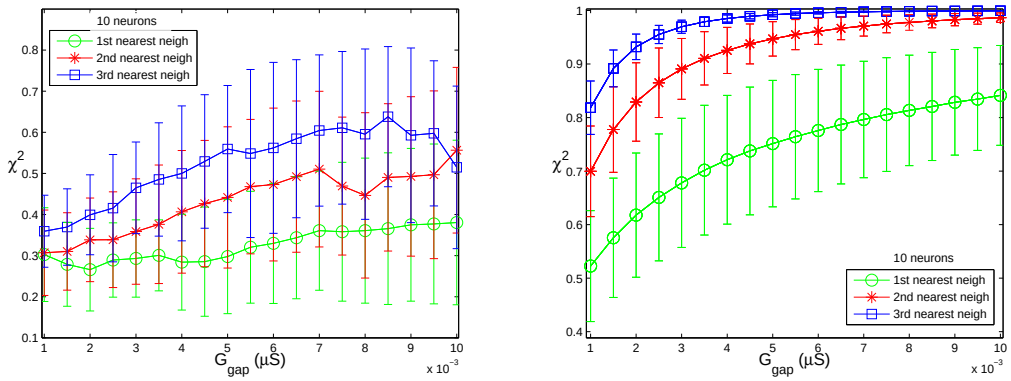

(a) (b)

Figure 5: χ^2 vs G_{gap} for networks with 10 neurons linked to their kth nearest neighbors (line is used for reference only). (a) For $I_{app} = 4.5$ nA the fluctuations are higher and χ takes very low values. For 3rd nearest neighbors the fluctuations are higher beyond $G_{gap} = 0.0075$ μS and whether the network reaches the state $\chi^2 = 1$ is not clear. (b) When $I_{app} = 6.0$ nA the functional dependence of χ^2 on the coupling strength G_{gap} is evident, and the behaviour is the same for networks with different number of neurons yet the more neighbors a neuron has, the faster the convergence to the value $\chi^2 = 1$ is. Each value has been averaged over 20 realizations where each of them runs 50000 iterations with a transient time of 10000.

in small-world topologies. To generate small-world networks we use the method proposed by Newmann and Watts [16]: Given a network with 20 neurons connected each to its 3rd nearest neighbors, for each connection a new link is added with probability p, therefore on average $20 \cdot 3p$ links are added, for this method neither loops nor repeated links are forbidden. For each value of p we average the value of χ^2 over 20 realizations.

The first case analyzes the relationship of χ^2 with three values of G_{gap}: 0.004 μS, 0.006 μS and 0.008 μS, by varying the probability p of adding new links to the network. The appled current is fixed to $I_{app} = 4.5$ nA. Although it is expected that for higher values of the coupling strength a higher value of the synchrony measure is obtained, it is interesting to notice the same behavior for all of the three cases, even though the randomness in the topology seems to be determinant since the functional dependance cannot be inferred straightforwardly: the minimum is reached for $p = 0.15$ and the maximum for $p = 0.95$, for example. In general, the values for $G_{gap} = 0.004$ μS remain below those for $G_{gap} = 0.006$ μS and the same occurs with this one and $G_{gap} = 0.008$ μS (See Fig. 6(a)).

The second case looks at the relation of the synchrony measure χ^2 with the applied current I_{app} and consequently the MMOs, indirectly. Three values of I_{app} are considered: $I_{app} = 4.3$ nA, $I_{app} = 4.5$ nA and $I_{app} = 6.0$ nA, for which the neurons have four, two and one MMO, respectively. The coupling strength is fixed to $G_{gap} = 0.004$ μS. For the highest current we observe that the dynamics on the network approaches to 1 which again suggests that the presence of more MMOs makes more difficult for the neurons to synchronize their firing. Fluctuations are higher for a current at $I_{app} = 4.3$ nA which oscillates around the values obtained for $I_{app} = 4.5$ nA.

*3.4. **Neurons in different regimes***

In this example we look at different topologies in which one neuron is in a different regime than the rest. We analyze one single network and the evolution of the network in time. We focus our attention on the time period where the network has reached a stable state. Additionally, we show the voltage traces for some neurons in the network.

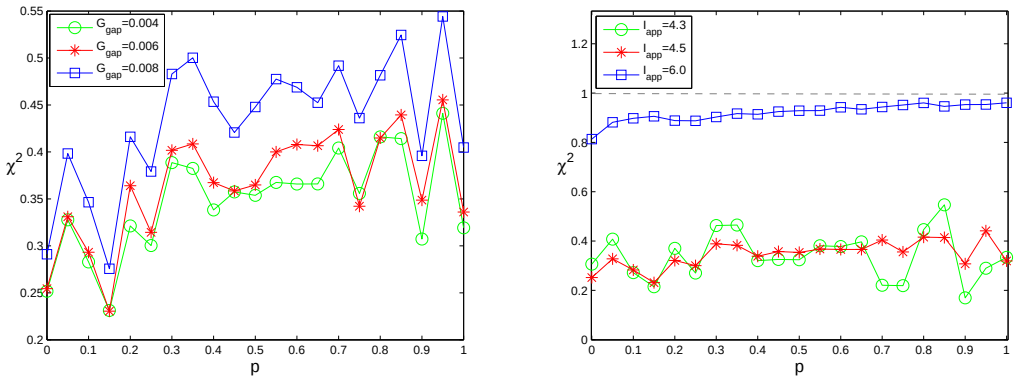

(a) (b)

Figure 6: (a) χ^2 vs probability p for small-world networks with 20 neurons for three different values of the coupling strength G_{gap}; I_{app} = 4.5 nA for all of them. For p = 0 we have networks whose neurons are connected to their 3rd nearest neighbors. (b) χ^2 vs probability p for small-world networks with 20 neurons for three different values of the applied current I_{app}; in the three cases G_{gap} = 0.004 μS. For regimes where we find more than one MMO, the fluctuations are high and the randomness in the topology has a stronger influence, whereas at I_{app} = 6.0 nA the value of χ^2 increases as the probability of adding new links increases. Each value has been averaged over 20 realizations where each of them runs 50000 iterations with a transient time of 10000.

3.4.1. ***Star topology***

The first case is a network with 6 neurons connected in a star topology. We fix the value of the coupling strength to G_{gap} = 0.006 μS. The only link between neurons is through the central neuron (neuron 1) which it happens to be in a different regime I_{app} = 4.3 nA. However, this central neuron drives the other neurons (in a regime I_{app} = 4.5 nA) to a state with same periodicity yet different phase. Some neurons fire during subprimary oscillations of others. Figure 7(a) shows the dynamics of the network for a small period of time. We observe than neurons 2, 3 and 4 fire simulateously, i.e. these neurons form a cluster, even though there is no direct link among them. The spikes of the other neurons that remain isolated are determined by the MMOs in the central neuron, which can be observed in Fig. 7(b) which shows the voltage trace for neurons in different clusters.

3.4.2. ***1st nearest neighbors***

The second case correspond to a network with 10 neurons coupled by their 1st nearest neighbors. Neuron 1 is in the regime I_{app} = 4.3 nA and the rest receive a slightly higher current of I_{app} = 4.5 nA. We find that the dynamics of the network converges to a state where all the neurons have the same period but different phase. Such a period is smaller than that of the uncoupled networks. The way neurons fire, it is highly related to the MMOs since the spike of some neurons take place during subprimary oscillations of others (See Figs. 8(a) and 8(b)).

3.4.3. ***Global coupling***

For a network of 10 globally coupled neurons three clusters are formed. Again neuron 1 is in a different regime and remains isolated. The other neurons form two clusters where neurons in a cluster fire simultaneously. Figure 9(a) shows the way neurons in the network organize; neurons in the clusters fire when the subprimary oscillations of neuron 1 take place. Figure 9(b) allows us to see the voltage trace of representative neurons for each cluster.

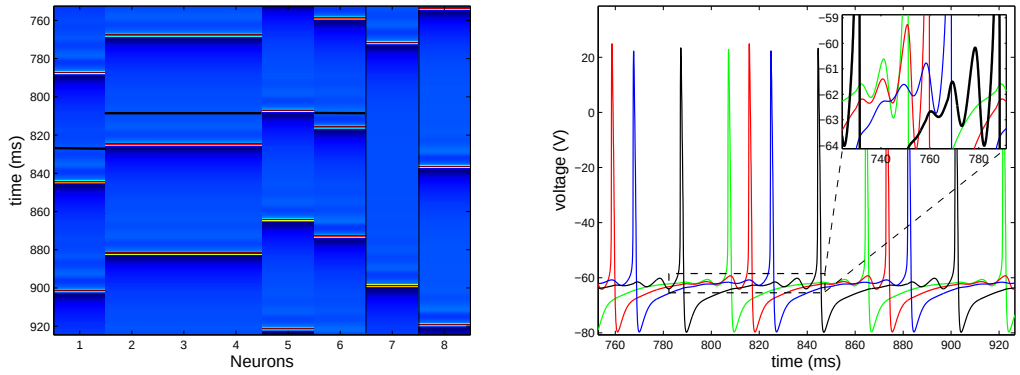

(a) (b)

Figure 7: (a) Evolution in time of a network with 6 neurons coupled in a star with the central neuron being in a regime at $I_{app} = 4.3$ nA (Neuron 1) and the rest at $I_{app} = 4.5$ nA. The coupling strength is $G_{gap} = 0.005$ μS. The spikes are observed in red. The rightmost neurons are uncoupled: Neuron 7 is in the regime $I_{app} = 4.3$ nA and Neuron 8 in $I_{app} = 4.5$ nA. The state which the network converges to shows clustering and the period of all the neurons is the same and smaller than the period in the uncoupled neurons. (b) Voltage trace for neuron 5 (green solid line), 6 (red solid line), 4 (blue solid line) and 1 (black solid line). MMOs in neuron 1 determine the phase at which following neurons fire.

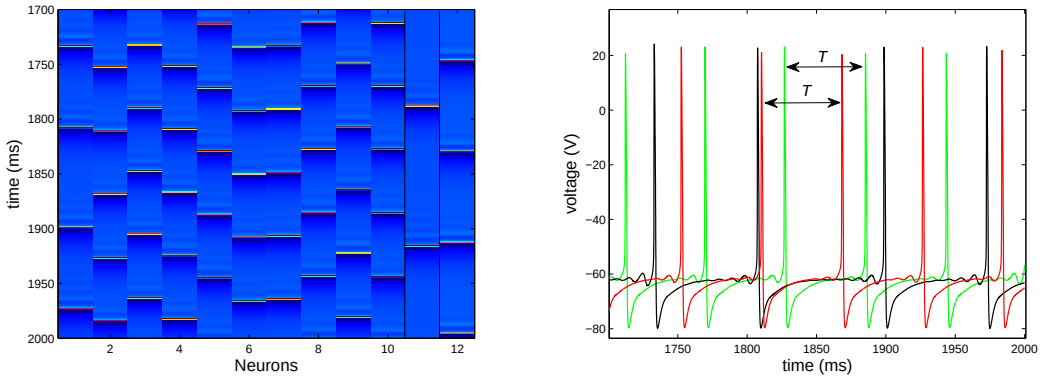

(a) (b)

Figure 8: (a) Evolution in time of a network with 10 neurons coupled to their 1st nearest neighbors. The coupling strength is $G_{gap} = 0.005$ μS. Neuron 1 is in a regime at $I_{app} = 4.3$ nA and the rest at $I_{app} = 4.5$ nA. The spikes are observed in red. The rightmost neurons are uncoupled: Neuron 11 is in the regime $I_{app} = 4.3$ nA and Neuron 12 in $I_{app} = 4.5$ nA. The state which the network converges to is such that neurons are not in phase but the inter-spike period is the same of all of those in the regime $I_{app} = 4.5$ nA. This period is smaller than the period in both uncoupled neurons. (b) Voltage traces for neurons 1 (black solid line) and its 1st nearest neighbors: neuron 2 (red solid line) and neuron 10 (green solid line). The period T of both neurons 2 and 10 is the same, and in general this is the same period at which all neurons in the regime $I_{app} = 4.5$ nA fire.

The role of MMOs in the dyamics of the networks becomes evident in the above examples. In this case, the neuron that is in a different regime, and in particular its MMOs, determine when the other neurons fire.

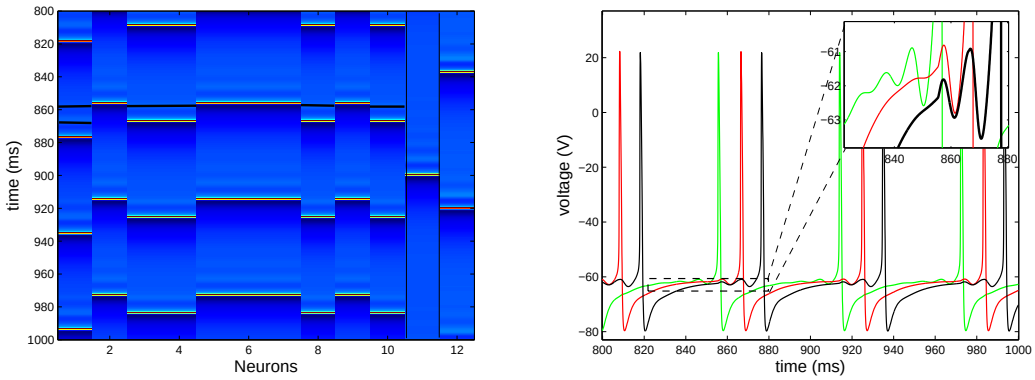

(a) (b)

Figure 9: (a) Evolution in time of a network with 10 neurons with all-to-all coupling. The coupling strength is $G_{gap} = 0.005\ \mu$S. Neuron 1 is at the regime $I_{app} = 4.3$ nA and the others are at $I_{app} = 4.5$ nA. The spikes are observed in red. The rightmost neurons are uncoupled: Neuron 11 is in the regime $I_{app} = 4.3$ and Neuron 12 in $I_{app} = 4.5$. Neuron 1 remains isolated whereas the other neurons self-organize in two clusters. (b) Voltage traces for neurons 2 (green solid line), 3 (red solid line) and 1 (black solid line). MMOs in neuron 1 determine when the other neurons in the netwrok fire. We observe that neuron 4 fires in phase with the last STO before the spike and neuron 6 fires in phase with the second last STO, for example.

4. Discussion

We have studied networks of motoneurons in different topologies. Electrical coupling between neurons, in general, tends to synchronize their firing, yet we can find clustering as well, especially in situations when neurons have several subprimary oscillations.

In globally coupled networks we were able to understand the influence of the coupling strength G_{gap} and the applied current I_{app} on the synchrony measure χ^2. For two neurons the convergence towards the value $\chi^2 = 1$, i.e. the complete synchronization, is different for the regimes $I_{app} = 4.5$ nA and $I_{app} = 6.0$ nA. In the first case, this convergence is slower than in the second case where it is reached for a medium coupling strength $G_{gap} = 0.005\ \mu$S. Surprisingly, for the regime $I_{app} = 6.0$ nA the functional dependence of χ^2 on G_{gap} is the same for networks with different number of neurons. It increases fast at the beggining and then it converges aymptotically to a completely synchronized state. In other words, more excitable motoneurons in the subprimary regime are more likely to synchronize their firing in comparison to less excitable cells.

When neurons are connected to their kth nearest neighbors their influence is just local. Therefore, this kind of networks allows us to study the importance of this local interaction for the overall behavior in the network. In a regime of $I_{app} = 4.5$ nA networks are very poorly synchronizable. The explanation is obvious, a local interaction does not allow to spread information efficiently and the time it takes for the network to synchronize is expected to be very long. The situation changes drastically for $I_{app} = 6.0$ nA. In this regime the dependence of χ^2 on the coupling strength G_{gap} grows asymptotically towards $\chi^2 = 1$ for all the networks studied. This suggests that for strong enough coupling the network synchronizes no matter how many neurons it has nor the number of neighbors these neurons are connected to.

Regarding small-world networks the randomness in the connections play an important role in the dynamics. In these examples we looked at the relationship between χ^2 and the probability p of adding new connections in the network. When networks with different coupling strength were studied and $I_{app} = 4.5$ nA fixed, we find a similar behavior: the minimum and maximum value of χ^2 are reached for the same

probability, $p = 0.15$ and $p = 0.95$, respectively. Moreover, the fluctuations decrease considerably when the probability is increased beyond $p = 0.25$. Nonetheless, for high probabilities beyond $p = 0.7$, the fluctuation among neurons become substantially higher and this is reflected in a decrease of the synchrony measure for some values of p. In contrast, for the relationship between χ^2 and the applied current I_{app} we fix the coupling strength to $G_{gap} = 0.004\ \mu$S we can just observe an asymptotic behavior for the case where $I_{app} = 6.0$ nA. When the neurons are in less excitable regimes it is much more difficult for them to synchronize.

An important observation must be made in relation to all these previous examples. The fact that the synchrony measure is less than one in most of the cases can certainly mean that the network forms clusters rather than synchronizes . However, one must bear in mind that this might also mean that the network does not converge to a stable dynamics in the time we ran the simulations, and therefore the network remains in a partially disordered configuration. Thus, we may also study the speed at which this stable configuration is attained.

The examples where neurons within the network are in different regimes give us insight about the role of the MMOs in the dynamics of the network. For this particular examples we observe that the neuron that is in a different regime does not synchronize and the others form clusters, in general. The inter-spike period of all the neurons in this network happened to be smaller than the period they would have had if they were uncoupled. Interestingly, the firing patterns were determined completely by the MMOs of the neuron in a different regime which suggests that these subprimary oscillations play a fundamental role in the overall behavior of a network of motoneurons. This examples could reflect a rather simplified situation in which a neuron, due to degenerative processes, becomes less excitable. The fasciculations observed in many patients can be regarded to this out-of-synchrony dynamics.

Comparison of these numerical results with experimental data could give us more insight into the biological mechanism by which networks of motoneurons behave the way they do and into the timescales real phenomena are produced. Hence, in the future this could have profound implications for human health in the treatment of degenerative motoneuron disorders.

Acknowledgments

I would like to express my gratitude to my supervisor Yulia Timofeeva for her valuable comments and support during the development of this project.

References

[1] R. J. Demarest C. R. Noback, N.L. Strominger and D. A. Ruggiero. *The human Nervous System. Structure and Function*. Humana Press, 2005.

[2] P. J. Shaw and M. J. Strong. *Motor Neuron Disorders*. Blue Books of Practical Neurology. Butterworth Heinemann, 2003.

[3] J. Desai M. Swash. Motor neuron disease: classification and nomenclature. *Amyotroph Lateral Scler Other Motor Neuron Disord*, 1:105–122, 2000.

[4] K. L. Bullinger M. Kraszpulski P. Nardelli F. J. Alvarez, H. E. Titus-Mitchell and T. C. Cope. Permanent central synaptic disconnection of proprioceptors after nerve injury and regeneration. *J Neurophysiol*, 106:2450–2470, 2011.

[5] M. Manuel-Y. Timofeeva N. Delestree C. Iglesias, C. Meunier and D. Zytnicki. Mixed mode oscillations in mouse spinal motoneurons arise from a low excitability state. *J Neurosci*, 31(15):5829–5840, 2011.

[6] A. A. Grace R. R. Lins and Y. Yarom. In vitro neurons in mammalian cortical layer 4 exhibit intrinsic oscillatory activity in the 10- to 50-hz frequency range. *Proc Natl Acad Sci USA*, 88:897–901, 1991.

[7] Y. Yarom Y. Gutfreund and I. Segev. Subthreshold oscillations and resonant frequency in guinea-pig cortical neurons: physiology and modelling. *J Physiol*, 483 (Pt 3):621–640, 1995.

[8] M. Donnet-F. Leroy C. J. Heckmann M. Manuel, C. Iglesias and D. Zytnicki. Fast kinetics, high-frequency oscillations, and subprimary firing range in adult mouse spinal motoneurons. *J Neurosci*, 29:11246–11256, 2009.

[9] B. Ermentrout and M. Wechselberger. Canards, clusters, and synchronization in a weakly coupled interneuron model. *SIAM J. Applied Dynamical Systems*, 8:253–278, 2009.

[10] N. Baba and K. Krischer. Mixed-mode oscillations and cluster patterns in an electrochemical relaxation oscillator under galvanostatic control. *Chaos*, 18:015103.

[11] O. Kiehn and M. Tresch. Gap junctions and motor behavior. *Trends Neurosci*, 25:108–115, 2002.

[12] B. Shraiman D. Golomb, D. Hansel and H. Sompolinsky. Clustering in globally coupled phase oscillators. *Phys. Rev. A*, 45:3516–3530, 1992.

[13] D. Hansel and H. Sompolinsky. Synchrony and computation in a chaotic neural network. *Phys. Rev. Lett.*, 68:718–721, 1992.

[14] D. Golom and J. Rinzel. Dynamics of globally coupled inhibitory neurons with heterogeneity. *Phys. Rev. E*, 48:4810–4814, 1993.

[15] I. Ginzburg and H.Sompolinsky. Theory of correlations in stochastic neuronal networks. *Phys. Rev. E*, 50:3171–3191, 1994.

[16] M. E. J. Newman. The structure and function of complex networks. *SIAM Review*, 45:167–256, 2003.